Pediatric Pulmonology 51:1284–1294 (2016)

Tools to Explore ABCA3 Mutations Causing Interstitial Lung Disease

Thomas Wittmann,[1] Ulrike Schindlbeck,[1] Stefanie Höppner,[1] Susanna Kinting,[1] Sabrina Frixel,[1] Carolin Kröner, MD,[1] Gerhard Liebisch, MD,[2] Jan Hegermann, PhD,[3] Charalampos Aslanidis, PhD,[2] Frank Brasch, MD,[4] Simone Reu, MD,[5] Peter Lasch, MD,[6] Ralf Zarbock, PhD,[1] and Matthias Griese, MD[1]*

Summary. Background: Interstitial lung diseases (ILD) comprise disorders of mostly unknown cause. Among the few molecularly defined entities, mutations in the gene encoding the ATP-binding cassette (ABC), subfamily A, member 3 (ABCA3) lipid transporter represent the main cause of inherited surfactant dysfunction disorders, a subgroup of ILD. Whereas many cases are reported, specific methods to functionally define such mutations are rarely presented. Materials and Methods: In this study, we exemplarily utilized a set of molecular tools to characterize the mutation K1388N, which had been identified in a patient suffering from ILD with lethal outcome. We also aimed to correlate in vitro and ex vivo findings. Results: We found that presence of the K1388N mutation did not affect protein expression, but resulted in an altered protein processing and a functional impairment of ABCA3. This was demonstrated by decreased dipalmitoyl-phosphatidylcholine (PC 32:0) content and malformed lamellar bodies in cells transfected with the K1388N variant as compared to controls. Conclusions: Here we present a set of tools useful for categorizing different ABCA3 mutations according to their impact upon ABCA3 activity. Knowledge of the molecular defects and close correlation of in vitro and ex vivo data will allow us to define groups of mutations that can be targeted by small molecule correctors for restoring impaired ABCA3 transporter in the future. **Pediatr Pulmonol. 2016;51:1284–1294.**

Key words: interstitial lung disease (ILD); respiratory distress syndrome and ARDS; surfactant biology and pathophysiology; neonatal pulmonary medicine; K1388N; ABCA3.

Funding source: DFG-970/8-1; chILD-EU, Number: FP7, No. 305653.

[1]Dr. von Hauner Children's Hospital, Ludwig-Maximilians University, German Centre for Lung Research, Munich 80337, Germany.

[2]Institute for Clinical Chemistry and Laboratory Medicine, University of Regensburg, Regensburg, Germany.

[3]Institute of Functional and Applied Anatomy, Hannover Medical School, German Center for Lung Research (DZL), Hannover, Germany.

[4]Department of Pathology, Academic Teaching Hospital Bielefeld, Bielefeld, Germany.

[5]Department of Pathology, Ludwig-Maximilians University, Munich, Germany.

[6]Pediatric Intensive Care, Hospital Bremen-Mitte, Bremen, Germany.

Thomas Wittmann and Ulrike Schindlbeck contributed equally to this work.

Conflict of interest: None.

*Correspondence to: Matthias Griese, MD, Dr. von Hauner Children's Hospital, Ludwig-Maximilians University, German Centre for Lung Research, Munich 80337, Germany. E-mail: Matthias.Griese@med.uni-muenchen.de

Received 23 January 2016; Revised 18 April 2016; Accepted 24 April 2016.

DOI 10.1002/ppul.23471
Published online 13 May 2016 in Wiley Online Library
(wileyonlinelibrary.com).

INTRODUCTION

ATP-binding cassette (ABC), subfamily A, member 3 (ABCA3) is an intracellular lipid transporter containing two transmembrane domains each consisting of six membrane helices and two nucleotide binding domains (NBDs) hydrolyzing ATP.[1,2] In the lungs, the transporter localizes to the outer membrane of lamellar bodies (LBs) of type II pneumocytes. LBs derive from lysosomal origin and serve as production and storage organelles for pulmonary surfactant, which is then secreted into the alveolar space. ABCA3 transports phospholipids and cholesterol into the LB lumen and is therefore essential for LB biogenesis and homeostasis of pulmonary surfactant and normal lung function.[1,3,4]

All these processes are delicately disturbed by sequence variations of *ABCA3*. A broad spectrum of mutations has recently been shown to cause pulmonary ABCA3 deficiency followed by early death or fibrotic lung disease in survivors.[5–8]

The deficiency of another ABC transporter, ABCC7 (Cystic fibrosis transmembrane conductance regulator, CFTR), shows many interesting similarities to ABCA3 deficiencies. The availability of cellular assays to characterize the CFTR phenotype in vitro and tight correlations to ex vivo patient data have led to the precise molecular classification of CFTR mutations,[9,10] successful correction of mutations in cell models with small molecules identified by high throughput screening and rapid transfer into patients.[11,12]

To acquire similar knowledge for ABCA3 deficiency, many intermediate steps need to be realized including stable and readily available cellular models, assays to characterize the cellular phenotype of the different mutations, and in particular close correlation of such measurements to ex vivo patient data. ABCA3 mutations, which were predicted to result in truncated or non-functional proteins were classified as "null" mutations.[8] If null mutations were present in homozygous or compound heterozygous states, the affected infants presented with respiratory failure at birth and all had died by 1 year of age in case not lung transplanted.[8] Mutations affecting protein function in any way were termed "other."[8] From a cellular perspective mutations were previously distinguished between those with abnormal localization of the ABCA3 protein in the cells and those with ATP hydrolysis defects.[1] The major role of ABCA3 in LB biogenesis and surfactant lipid synthesis, that is, dipalmitoyl-phosphatidylcholine (PC 32:0) content of the cells, must also be considered.[13,14]

Such cellular classifications of ABCA3 mutations have to be linked to the clinical characterizations of affected subjects carrying different types of *ABCA3* gene sequence variations to build up a consistent and reliable model.

In this study, we used a broad range of experiments to assess in vitro and ex vivo characteristics of wild type and a mutated ABCA3 protein. Our results demonstrate a very close connection between the results obtained in the cell model applied and the findings from a patient harbouring the same homozygous ABCA3 variant. The molecular tools defined here allow a classification of ABCA3 mutations; this will be of use when searching for new molecules to restore genetically disturbed ABCA3 function.

MATERIALS AND METHODS (SEE DETAILED DESCRIPTIONS IN THE SUPPLEMENTAL MATERIAL)

Plasmids and Antibodies

ABCA3 cDNA (NM_001089) fused to a C-terminal HA-tag and puromycin resistance gene were cloned into pT2/HB transposon vector (Addgene, Cambridge, plasmid #26557). ABCA3-K1388N point mutation (c. 4164G>C; AAG/AAC) was introduced using Q5® site-directed mutagenesis kit (NEB, Ipswich, MA) with following primers: K1388N-for *5′-AGCTCTCCAACGTGTAC-GAGC-3′* and K1388N-rev *5′-CCTTGATAATCA-GAGGTGTG-3′*. pCMV(CAT)T7-SB100 transposase was ordered from Addgene (plasmid #34879).

Used antibodies are listed in the supplement.

Cell Culture

A549 cells were purchased from the German Collection of Microorganisms and Cell Cultures (DSMZ, Braunschweig, Germany) and maintained in RPMI 1640 medium (Gibco, Darmstadt, Germany) supplemented with 10% fetal bovine serum (FBS) (Sigma, Taufkirchen, Germany) at 37°C with 5% CO_2.

Generation of Stable Cell Clones

ABCA3-HA wild type (WT) and K1388N variation were stably transfected using the "*Sleeping Beauty*" transposon system.[15] Therefore, A549 cells were co-transfected with pCMV(CAT)T7-SB100 and pT2/HB-puro-ABCA3-HA WT or K1388N variation using X-tremeGENE HP DNA transfection reagent (Roche, Mannheim, Germany). Selection of stable cells was started by addition of 1 μg/ml puromycin.

Viability and Cytotoxicity Assay

Cell viability was assessed by specific cleavage of 2,3-bis (2-methoxy-4-nitro-sulfophenyl)-2H-tetrazolium-5-carboxyanilide (XTT, Sigma) in the presence of phenazine methosulfate. Absorbance was measured at 490 and 650 nm using a spectrophotometer.

For cytotoxic effects of stable transfection, the amount of lactate dehydrogenase (LDH) was determined in cell supernatants according to the manufacturer's instructions (Promega, Mannheim, Germany).

Real-Time PCR/Immunoblotting/ Immunofluorescence Staining/Oil Red O Staining

Real-time PCR, immunoblotting, immunofluorescence staining, and oil red O staining were performed as previously described.[16] To determine cellular oil red O volume, Z stacks image series were generated with an Olympus IX81/Fluoview FV1000 confocal laser scanning microscope (Olympus, Tokyo, Japan). Data were analyzed with the 3D object counter software plugin in ImageJ.

Glycosylation Analysis/Lipid Analysis/Electron Microscopy

Glycosylation analysis was done as previously described.[1] Lipid analysis in bronchoalveolar lavages (BAL) was performed as previously reported.[14] For lipid analysis, cells were seeded at 200,000 cells per 6-well using Quantum 286 Complete Epithelial Medium (PAA) without addition of FBS. Cells were grown for 48 hr. After that time, the supernatant was collected, pooled, and concentrated using a SpeedVac. Cells were washed with PBS twice and lysed in SDS buffer (0.1% SDS, 1 mM EDTA in 0.1 M Tris pH 7.4) at room temperature. Lipids were extracted from cells and concentrated supernatant as previously described by ESI-MS/MS in positive ion mode.[14] Altered lipid profiles were verified in additional disease controls (data not shown). Electron microscopy was performed as described.[7]

Vesicle Volume

A549 cells containing either ABCA3-WT or K1388N variation were immunostained against HA-tag and imaged with an Olympus IX81/Fluoview FV1000 confocal laser scanning microscope. Diameter of ABCA3-HA containing vesicle was determined with ImageJ software. Volumes of 60 different randomly chosen vesicles from three different experiments were calculated. Therefore, 20 vesicles from 10 different cells were analyzed per experiment. Vesicles were reviewed by a pathologist specialized for lamellar body characterization.

Immunohistochemistry

Slides were pretreated with Target Unmasking Fluid (Panpath, Amsterdam, The Netherlands) at 90°C followed by an incubation of primary antibody against ABCA3 protein (diluted 1:1800) for 60 min at RT. Detection was done using Vectastain ABC-Kit Elite Universal (Vector Laboratories, Burlingame) and AEC+ chromogen as substrate (Dako, Santa Clara). Slides were counterstained with Hematoxylin Gill's Formula (Vector Laboratories). Microscopic pictures were taken with a Leica DM4000 (Leica, Wetzlar, Germany).

In Vivo and Ex Vivo Analysis of Patient Materials

BAL, lung tissue, and blood were investigated from an infant. Informed consent of the parents and approval of the institutional review board (EK 026-06) were obtained. Analysis of data was performed under the FP7-305653 project chILD-EU (EK 111-13).

Statistical Analysis

Comparison of two groups was done using Student's *t*-test. Comparisons of multiple groups were done using one-way repeated measure ANOVAs with Tuckey's post hoc test. Analysis of lipid classes was done using two-way ANOVA with Sidak's post hoc test. P-values < 0.05 were considered to be statistically significant. The ratios of phosphatidylcholine species were analyzed using one-sample *t*-test comparing to the hypothetical value of 1. Followed this, a new significance level was calculated according to Benjamini and Hochberg.[17] Results were presented as mean $\pm$ S.E.M. of a minimum of three different experiments.

RESULTS

The Homozygous K1388N Variant of ABCA3 Protein Leads to Complete ABCA3 Deficiency Resulting in Lethal Interstitial Lung Disease

The homozygous ABCA3 variation K1388N was found in a patient presenting typically for complete ABCA3 deficiency with severe respiratory distress (Fig. 1A and B), a brief period of recovery with interstitial lung disease and the typical histological pattern of chronic pneumonitis of infancy and abnormal LB on electron microscopy (Fig. 1C–F), progressing to respiratory insufficiency and death at the age of 9 weeks. SP-C content of BAL was reduced and showed some higher molecular weight forms at relatively low concentration (Fig. 1G). This is concordance with previous studies, which showed reduction of SP-C protein in BALs from patients with ABCA3 deficiency.[18–20] The K1388N mutation was predicted to be malign and not tolerated by the algorithms Polyphen and SIFT. A topological model of ABCA3 protein predicts a localization of K1388N variant in proximity to the nucleotide-binding domain 2 (NBD2) (Fig. 1H), which comprises two Walker motives.[21] Furthermore partial alignment of codons 1348-1429 of the ABCA3 coding sequence demonstrates an extremely conserved region including Lys1388 between different species (Fig. 1I).

Impaired Intracellular Processing of K1388N Variation

A549 lung epithelial cells stably expressing ABCA3-WT and ABCA3-K1388N variant showed an increased

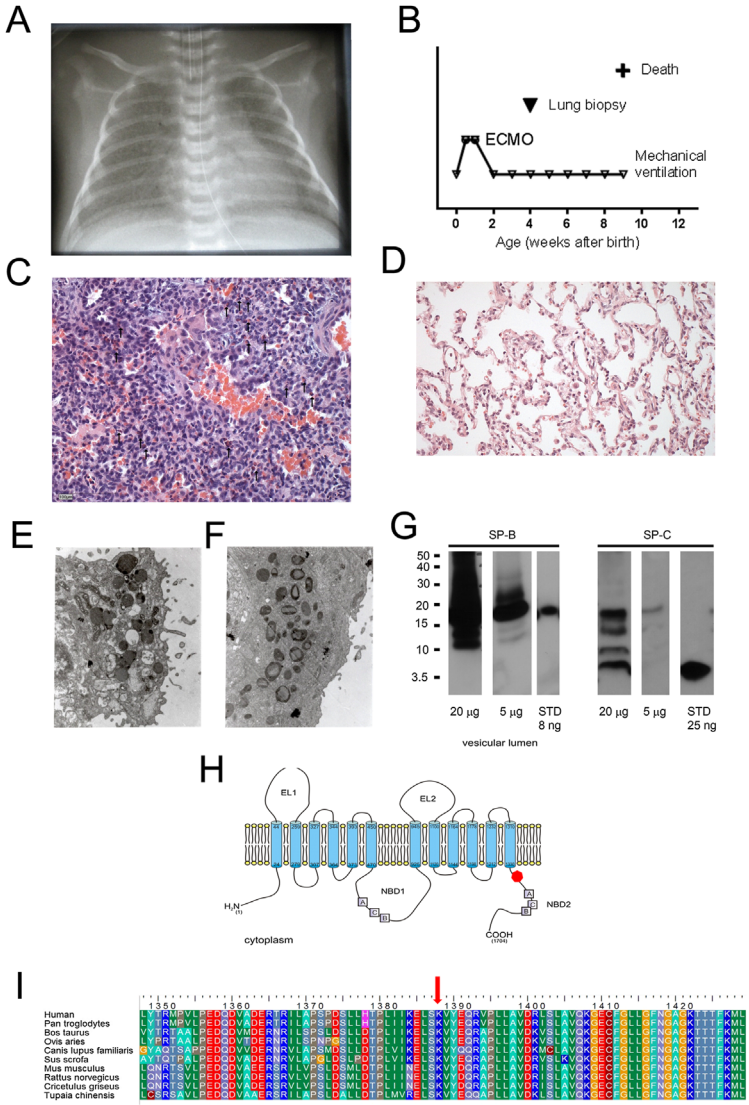

Fig. 1. Clinical characterization of a child carrying homozygous K1388N variation of ABCA3 protein. (A) Chest x-ray: Initial chest x-ray showing homogenous fine reticular ground glass opacification. (B) Clinical course of the neonate (ECMO = extra corporal membrane oxygenation). (C) Lung biopsy: Lung biopsy showing the pattern of chronic pneumonitis of infancy; note increased presence of eosinophils (indicated by small block arrows, scale indicates 100 µm); for comparison a normal biopsy is given in D. E and F shows electron micrographs demonstrating plenty, albeit abnormal lamellar bodies in type II cells (magnification 20,000×). No normal appearing lamellar bodies were identified in the patient. Note the lack of lamellar structures and the presence of aggregates of dense material located marginally. (G) Western blotting of a tracheobronchial aspirate (SP-B and SP-C), indicated amount of total protein of lavage added per lane and the respective standards (STD) of the patient obtained at the age of 5 weeks of life, 4.8 weeks after the administration of a single dose of exogenous surfactant. After SDS–PAGE and transfer, the membranes were probed with antibodies against SP-B and SP-C. Molecular weights (kDa) are indicated on the left side. All bands were analyzed under non-reducing conditions. SP-B was detected in large amounts (compare to standard STD of 8 ng applied to lane 2). In addition to the typical bands at 18 kDa some lower bands (monomers or degradation products), as well as higher molecular forms were observed. SP-C was detected in relatively smaller amounts making up <10% of the total amount of SP-C (usually about 50%). Of interest was the presence of several higher molecular weight bands; this pattern is typically seen in patients with alveolar proteinosis. H. Schematic representation of ABCA3 protein with different sequence motifs and correct orientation. The K1388N mutation is shown as red filled hexagon. I. Partial amino acid alignment of ABCA3 sequences (codons 1348-1429). Alignment is showing that Lys1388 (indicated by red arrow) is extremely conserved.

ABCA3-mRNA expression of 200-fold as compared to mock transfected cells (Fig. 2A). Furthermore cell growth and proliferation were unaffected in both cell lines either expressing ABCA3-K1388N or ABCA3-WT protein in comparison to mock control cells (Fig. 2D + E). But intracellular processing examined by Western immunoblotting revealed an alteration of K1388N variant compared to wild type protein (Fig. 2B). Both proteins were present as the 190 and 150 kDa processing forms, but band intensities differed. The 190 kDa processing

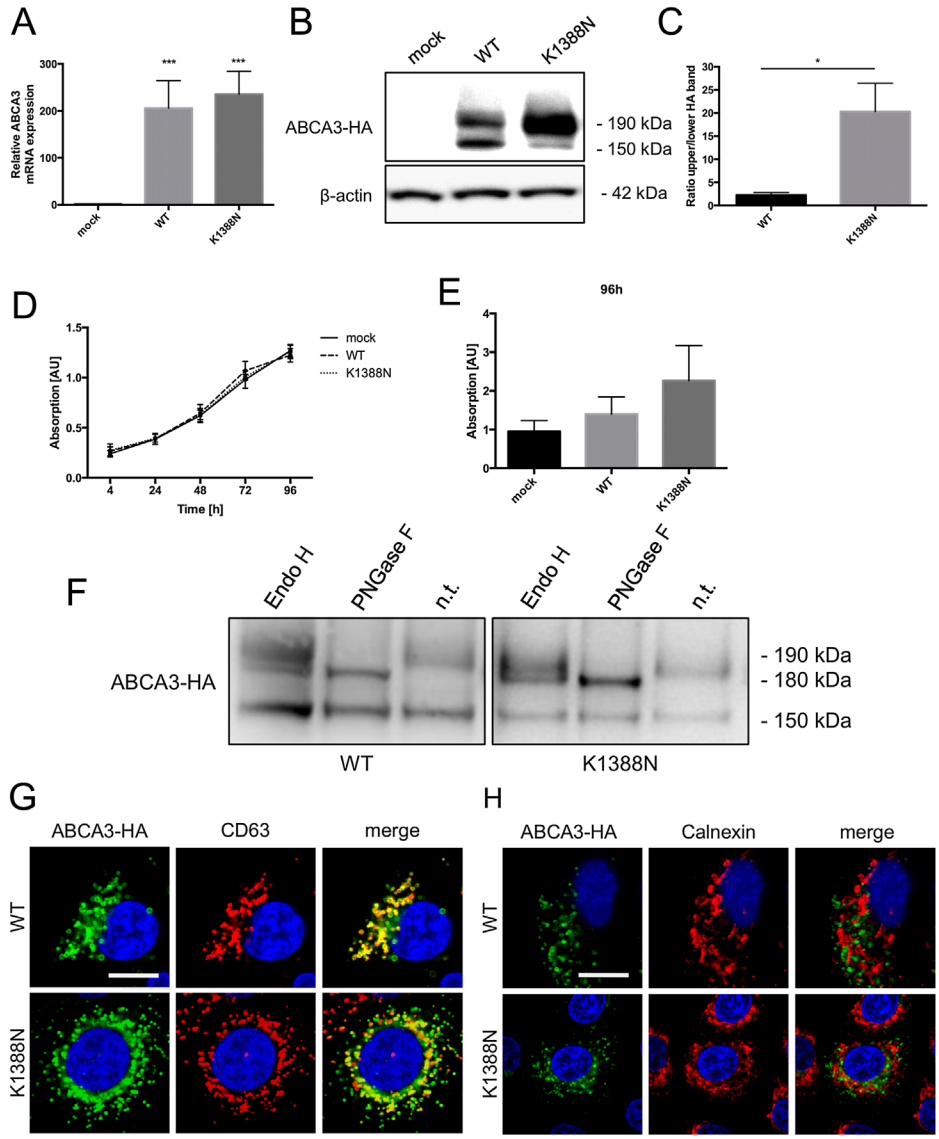

Fig. 2. Cellular effects of ABCA3-WT and ABCA3-K1388N stably expressed in A549 cells. (A) ABCA3 mRNA levels analyzed by quantitative real time PCR ($P < 0.001$ for WT/mock and K1388N/mock). (B) Western immunoblot analysis of HA-tagged ABCA3 in total cell lysates. β-actin was used as a loading control. (C) Ratio of upper/lower ABCA3 processing form ($P < 0.5$). (D) Cell proliferation assay of A549 cells stably transfected with WT and K1388N mutated ABCA3 protein compared to mock control. XTT tetrazolium salt was used for absolute quantification. (E) Impact of stably transfection method on cell cytotoxicity. Therefore lactate dehydrogenase was quantified in cell supernatants. (F) N-Glycosylation of ABCA3-HA WT and K1388N protein. The noncleaved 190 kDa ABCA3-HA protein is fully deglycosylated by PNGase F causing a shift in electrophoretic mobility to 180 kDa. Endo H digestion results in a separation of Endo H-sensitive 180 kDa ABCA3-HA protein (containing only high-mannose oligosaccharides) and Endo H-insensitive 190 kDa ABCA3-HA protein (with complex-type oligosaccharides). (G) Co-immunostaining of HA-tagged ABCA3 with the lysosomal (lamellar body) marker CD63. (H) Co-immunostaining of HA-tagged ABCA3 with the ER marker calnexin (scale: 10 μm).

form of the mutated K1388N protein was enriched considerably. Therefore, the band ratio of 190–150 kDa was increased up to 20-fold in ABCA3-K1388N expressing cells as compared to A549 cells with ABCA3-WT protein (Fig. 2C). Intracellular processing examined by co-localization studies with the immunofluorescent marker CD63, a marker for late endosomes and lamellar bodies, revealed localization within CD63 positive vesicles of both wild type and K1388N protein variant (Fig. 2G). Furthermore neither ABCA3 wild type protein nor K1388N mutated protein showed a co-localization with the ER-resident chaperone calnexin (Fig. 2H). Additional N-glycosylation studies revealed that ABCA3 wild type protein as well as K1388N mutated protein showed equal processing from high-mannose oligosaccharides to complex-type oligosaccharides (Fig. 2F). This further supports the view that both proteins undergo correct folding in the ER and further processing within the Golgi apparatus.

K1388N Variation Results in Smaller Lamellar Bodies With Abnormal Morphology

Analysis of ABCA3-K1388N containing lamellar bodies revealed a significant decrease of volume compared to lamellar body volume of A549 cells expressing ABCA3-WT (Fig. 3A). Lamellar body morphology of ABCA3-K1388N expressing cells was altered as compared to ACBCA3-WT expressing cells. Mock control cells contained no lamellar bodies (Fig. 3B, left), whereas ABCA3-WT expressing cells showed well-structured lamellar bodies with concentric membranes arranged in parallel (Fig. 3B, middle). ABCA3-K1388N containing lamellar bodies showed abnormal morphology with fried-egg-like structures (Fig. 3B, right). Additional analysis of lung tissue from a patient carrying homozygous K1388N variant showed a very weak expression and a high dispersed ABCA3 protein in type II pneumocytes, whereas ABCA3 is strongly expressed in healthy lung tissue (Fig. 3C). Control tissue displayed a typical pattern of LBs with ring-like structures, whereas LBs in lung tissue with ABCA3-K1388N variant were absent (compare Fig. 3C left to right).

Reduction of Phosphatidylcholine and Dipalmitoyl-Phosphatidylcholine Content Due to K1388N Mutation

Measurement of intracellular lipid classes from A549 cells expressing ABCA3-K1388N mutated protein exhibits a reduction of phosphatidylcholine content as the major lipid in surfactant compared to A549 cells expressing ABCA3-WT (Fig. 4A, left). Other lipid classes were not affected by this mutation (Supplemental Fig. S1A, right). Free cholesterol content and cholesteryl esters were significantly reduced in K1388N expressing A549 cells, whereas lipid droplet volume and lipid droplet number showed no differences compared to A549 expressing ABCA3-WT cells (Supplemental Fig. S2A + B). On the detailed PC species level short-chained lipid contents were reduced in contrast to long-chained species, which were increased (Supplemental Fig. S1B, right). PC 32:0 as the most abundant PC species in surfactant was also reduced to a third (Fig. 4A, right). These findings can also be verified in BAL isolated from the homozygous carrier of the K1388N variant. PC content was also lowered as compared to BALs of control group (Fig. 4B, left). Additionally sphingomyelin (SPM), PE based plasmalogens (PE P), and phosphatidylglycerol (PG) content were decreased, whereas ceramide (Cer) content was slightly increased (Supplemental Fig. S1A, left). This was not observed in A549 cells expressing ABCA3-WT compared to ABCA3-K1388N (Supplemental Fig. S1A, right). Furthermore molecular PC species composition showed a similar distribution with a lower fraction of PC 30 and 32 species and more PC 36 and 38 species compared to controls (Supplemental Fig. S1B, left). PC 32:0 content of a patient with K1388N variation was diminished by half of it as compared to controls (Fig. 4B, right).

DISCUSSION

In this study, we present a broad set of experiments to assess the function of wild type ABCA3 protein in comparison to the specific features of ABCA3 with the mutation K1388N, which was found in a patient suffering from respiratory distress syndrome (Table 1). Our goal was to establish different molecular tools for the characterization and classification of newly described ABCA3 variants and to test the tightness of correlation between the in vitro data raised in stably transfected A549 cells and ex vivo data collected from an affected subject.

The K1388N variation of the ABCA3 transporter caused severe respiratory neonatal distress followed by a brief period of recovery with interstitial lung disease, progressing to respiratory insufficiency and death at the age of 9 weeks. Obviously, this newly described homozygous mutation led to complete ABCA3 deficiency, which is incompatible with life.[22] In silico analysis predicted these damaging consequences of this mutation, which is localized in proximity of the functional critical nucleotide-binding domain 2 (NBD2). Lys1388 is a highly conserved position among various species, further supporting its role for normal function of ABCA3 protein.

It could be shown for some ABC transporters like ABCC7 (CFTR) that certain mutations induce intracellular mislocalization of the protein.[23,24] Our data clearly show that ABCA3-K1388N is correctly localized to lamellar bodies and was not retained in the ER.

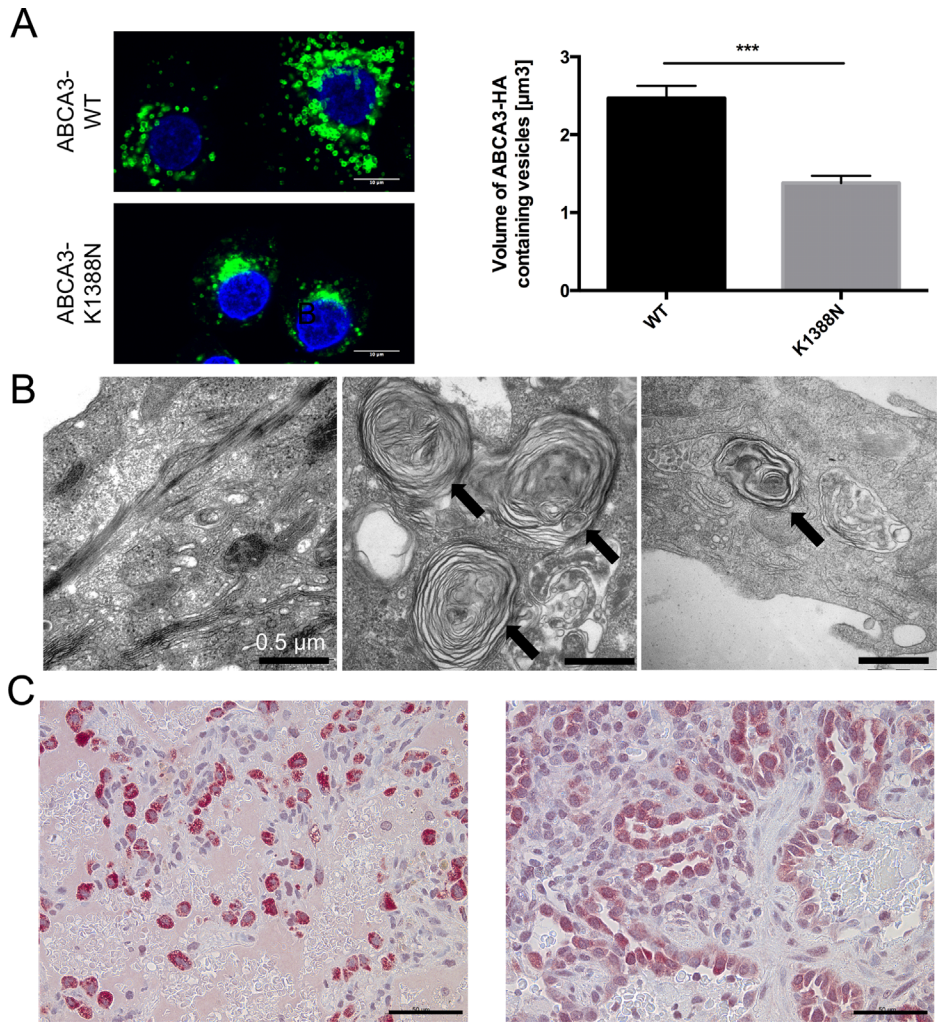

Fig. 3. Impact of ABCA3-K1388N variant on lamellar body volume and morphogenesis. (A) Left: immunofluorescence staining of HA-tagged ABCA3-WT and ABCA3-K1388N protein included in vesicles (scale: 10 μm). Vesicle volume was calculated based on diameter. Right: mean values of vesicle volumes containing either ABCA3-WT or ABCA3-K1388N protein. $^{***}P < 0.001$. (B) Electron microscopy of lamellar bodies showing mock control (left), ABCA3-WT (middle), and ABCA3-K1388N expressing A549 cells (right), respectively. Mock control cells contained no lamellar bodies, whereas ABCA3-WT transfected cells obtained morphological well-shaped LB with concentric membranes arranged in parallel (middle, black arrows). ABCA3-K1388N transfected A549 cells showed abnormal, fried-egg like structured lamellar bodies (right, black arrows). Scale: 0.5 μm. (C) Immunohistochemical staining of ABCA3 protein in lung tissues. Lung tissue of a healthy control patient expressing ABCA3 protein (left, red staining). ABCA3 expression shows strong staining intensity and typical pattern of ring-like structures located in the cytoplasm of type II pneumocytes. Right: ABCA3 protein expression in lung tissue of patient with homozygous ABCA3-K1388 K protein variant. Very weak staining intensity and diffuse distribution of ABCA3 protein in type II pneumocytes can be detected (scale: 50 μm).

Remarkably, other well-described ABCA3 variants like L101P led to an altered protein processing and a disturbed protein trafficking.[1] The processing of its oligosaccharides from the high mannose type to the complex type showed trafficking through ER and Golgi apparatus. This follows the cellular path of ABCA3-WT protein, which also passes through these two organelles. Nevertheless, cellular processing of K1388N is impaired compared to WT protein, as the 190 kDa processing form of the protein is enriched in A549 cells stably expressing the variant. Although overexpression of the 190 kDa processing form tends to affect trafficking, the K1388N variant is located to LBs.[25,26] Previous studies showed that N-glycosylation is essential for the stability of ABCA3 protein.[21] Introducing a further N-glycosylation site due to another asparagine instead of a lysine on position 1,388 may lead

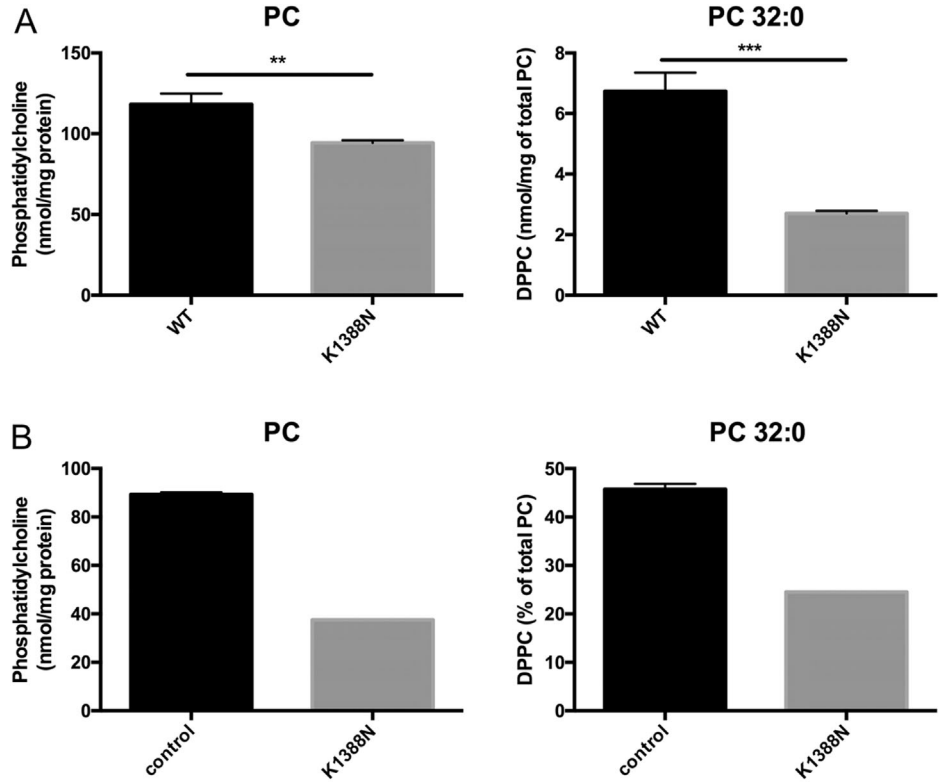

Fig. 4. PC and PC 32:0 content. (A) Intracellular PC and PC 32:0 content of A549 cells carrying ABCA3-K1388N variant compared to that in cells expressing ABCA3-WT protein. $^{**}P < 0.01$, $^{***}P < 0.001$. (B) PC and PC 32:0 content in BAL of patient with homozygous ABCA3-K1388N mutation compared to control group.

to elevated protein instability. Thus several lines of evidence support impaired processing of the K1388N variant most likely resulting in less active transporter available and may therefore lead to reduced volume and structurally altered LBs. Whereas, ABCA3-WT expression led to the prominent induction of well-shaped LBs in A549 cells, expression of ABCA3-K1388N induced the formation of abnormal LBs. This notion supports the concept that ABCA3 wild type function is indispensable for normal LB production and that this ability is severely impaired in the K1388N variant.

Analysis of lung tissue from the child carrying the homozygous K1388N variant demonstrated an altered expression pattern of ABCA3 protein in type II pneumocytes. This was identified by a weak immunohistochemical staining of ABCA3 and only rather small protein agglomerations compared to normal well-shaped LBs detectable in tissues from healthy children. Similarly, in lung tissue investigated from the affected child, the characteristic fried-egg-shaped and functionally inactive, but no normal LBs were demonstrated. Together, we show a close recapitulation of morphological LB dysfunction in our stable cell model and the patient.

To directly assess the functional impact of the K1388N variant compared to ABCA3-WT protein, lipid composition was measured. Previous studies showed that the amount of PC 32:0 is significantly reduced in BALs of children carrying interstitial lung disease causing mutations on both alleles.[13,14] Both total PC and PC 32:0 were reduced in A549 cells stably expressing ABCA3-K1388N and in BAL of the child with homozygous K1388N variant compared to respective controls. This provides direct in vitro and ex vivo evidence for reduced ABCA3 lipid transporter function. Furthermore the K1388N variant led to an elevation of long-chained PC species content in both A549 cells and in BAL of the patient compared to controls. Previous studies showed that ABCA3 variants cause defects in ATP hydrolysis.[1] It remains to be determined, whether the K1388N variant leads to decreased lipid transport due to impaired ATP hydrolysis. The lipid profile of K1388N variant was more similar to the hydrolysis mutation E292V (data not shown).

Whereas a major strength of our study was to correlate the in vitro data from our model system for lung epithelial cells and ex vivo data from a patient in relation to the K1388N variant, there are some weaknesses. We assessed intracellular lipid composition; however, the surfactant lipids are usually exocytosed into the alveolar space in vivo and thus represent just a subfraction. We found a

TABLE 1— Criteria and Molecular Tools Used to Characterize the ABCA3 Transporter

Criterion for classification	Molecular tool	Mock transfected cells/healthy controls	ABCA3-WT cells	Difference *P*-value	ABCA3-K1388N cells/patient	Difference *P*-value
Processing (Ratio 190/150 kDa form)	Western blot	n.a.	2.26 ± 0.30	n.a.	20.30 ± 3.55	0.0316**
Intracellular protein localization	Immunofluorescence	n.a.	Co-localization with CD63	—	Co-localization with CD63	—
	Immunohistochemistry in patient tissue sections	Strong and ring-like ABCA3 staining in type II pneumocytes	n.a.	—	Weak and dispersed ABCA3 staining pattern in type II pneumocytes	—
Intracellular trafficking	N-glycosylation analysis	n.a.	Trafficking through ER and Golgi apparatus	—	Trafficking through ER and Golgi apparatus	—
Lamellar body volume	Immunofluorescence	n.a.	2.47 ± 0.16	n.a.	1.38 ± 0.10	<0.0001**
Lamellar body morphogenesis	Electron microscopy	Scarce or no lamellar bodies	Well-shaped lamellar bodies with concentric membranes	—	Abnormal fried-egg like shaped lamellar bodies	—
Phosphatidylcholine content A549 cells (nmol/mg protein) (n = 9)	Mass spectrometry	90.11 ± 0.97	118.25 ± 6.52	0.0061*	94.31 ± 1.57	0.1340* 0.0101***
Phosphatidylcholine content BAL (% of all analyzed phospholipids)		89.3 ± 0.8	n.a.	n.a.	37.5	n.a.
Dipalmitoyl-phosphatidylcholine (PC 32:0) content A549 cells (nmol/mg protein) (n = 9)		4.52 ± 0.05	6.74 ± 0.61	0.0235*	2.70 ± 0.09	<0.0001* 0.0003***
Dipalmitoyl-phosphatidylcholine (PC 32:0) content BAL (% of all PC species)		45.8 ± 1.1	n.a.	n.a.	24.5	n.a.

n.a., not available. Mean values (±S.E.M.) are displayed (Student's *t*-test and one-way repeated measure ANOVAs with Tuckey's post hoc test were used).

**P*-values compared to control.

***P*-values compared to ABCA3-WT.

****P*-values ABCA3-K1388N compared to ABCA3-WT.

tight correlation for PC 32:0 which, as the major surfactant phosphatidylcholine species is enriched in lamellar bodies.[27] We expected this in vitro, but the sensitivity of mass spectrometry to determine unlabelled PC 32:0 directly in the supernatant of cells cultured in dishes was too low. However, an enrichment of intracellular PC 32:0 was shown in our model system.

Patient-derived type-II-pneumocytes would be most helpful for in vitro studies on specific mutations; however, such lines are not available for most rare mutations.[28,29] The A549 cell-line used here was formerly derived from lung adenocarcinoma and lost its ability to form LBs with normal structure and characteristic surfactant composition.[30] However, this may even be of advantage to demonstrate transport of surfactant lipids into such organelles in vitro. Here we show that the expression of ABCA3-WT protein at a constantly high level led to the formation of well-shaped LBs with an enrichment of PC and PC 32:0 content. This morphological feature has previously been shown for HEK293 cells[3,7] and represents an elegant functional assay for intact ABCA3 transporter activity.

Collecting further clinical data from patients with this mutation linked to laboratory-based experiments to understand how a particular mutation works will be necessary and will be of use for allocating mutations into groups with the same class of a molecular defect in the future. This is essential in face of the large number of different ABCA3 mutations identified, as those from the same class might be targeted by the same group of small

molecules for restoring the wild type function of the protein.

In summary, we characterized the K1388N variant of ABCA3 as a processing mutation with normal intracellular localization and a reduced lipid transporter activity for PC 32:0. This led to LBs with a reduced volume and an abnormal morphology. Thus this mutation can be classified as a functional mutation.

ACKNOWLEDGMENTS

The work of M.G. was supported by DFG-970/8-1 and chILD-EU (FP7, No. 305653).

AUTHORS' CONTRIBUTION

Thomas Wittmann, Ulrike Schindlbeck, Ralf Zarbock, Matthias Griese designed the study, analyzed data, wrote the manuscript. Thomas Wittmann, Ulrike Schindlbeck, Stefanie Höppner, Susanna Kinting, Sabrina Frixel, Simone Reu, Gerhard Liebisch, Jan Hegermann performed research, contributed important reagents, analyzed data. Matthias Griese, Peter Lasch, Charalampos Aslanidis, Frank Brasch, Carolin Kröner evaluated the patient, made chart reviews, organized the study logistics. All authors approved the final manuscript. Matthias Griese is responsible for the study content, validity of the data.

REFERENCES

1. Matsumura Y, Ban N, Ueda K, Inagaki N. Characterization and classification of ATP-binding cassette transporter ABCA3 mutants in fatal surfactant deficiency. J Biol Chem 2006;281: 34503–34514.
2. Peca D, Cutrera R, Masotti A, Boldrini R, Danhaive O. ABCA3, a key player in neonatal respiratory transition and genetic disorders of the surfactant system. Biochem Soc Trans 2015;43: 913–9.
3. Cheong N, Zhang H, Madesh M, Zhao M, Yu K, Dodia C, Fisher AB, Savani RC, Shuman H. ABCA3 is critical for lamellar body biogenesis in vivo. J Biol Chem 2007;282:23811–23817.
4. Besnard V, Matsuzaki Y, Clark J, Xu Y, Wert SE, Ikegami M, Stahlman MT, Weaver TE, Hunt AN, Postle AD, et al. Conditional deletion of Abca3 in alveolar type II cells alters surfactant homeostasis in newborn and adult mice. Am J Physiol Lung Cell Mol Physiol 2010;298:L646–L659.
5. Shulenin S, Nogee LM, Annilo T, Wert SE, Whitsett JA, Dean M. *ABCA3* gene mutations in newborns with fatal surfactant deficiency. N Engl J Med 2004;350:1296–1303.
6. Saugstad OD, Hansen TW, Ronnestad A, Nakstad B, Tollofsrud PA, Reinholt F, Hamvas A, Coles FS, Dean M, Wert SE, et al. Novel mutations in the gene encoding ATP binding cassette protein member A3 (*ABCA3*) resulting in fatal neonatal lung disease. Acta Paediatr 2007;96:185–190.
7. Campo I, Zorzetto M, Mariani F, Kadija Z, Morbini P, Dore R, Kaltenborn E, Frixel S, Zarbock R, Liebisch G, et al. A large kindred of pulmonary fibrosis associated with a novel *ABCA3* gene variant. Respir Res 2014;15:43.
8. Wambach JA, Casey AM, Fishman MP, Wegner DJ, Wert SE, Cole FS, Hamvas A, Nogee LM. Genotype-phenotype correlations for infants and children with ABCA3 deficiency. Am J Respir Crit Care Med 2014;189:1538–1543.
9. Sosnay PR, Siklosi KR, Van Goor F, Kaniecki K, Yu H, Sharma N, Ramalho AS, Amaral MD, Dorfman R, Zielenski J, et al. Defining the disease liability of variants in the cystic fibrosis transmembrane conductance regulator gene. Nat Genet 2013;45:1160–1167.
10. Okiyoneda T, Veit G, Dekkers JF, Bagdany M, Soya N, Xu H, Roldan A, Verkman AS, Kurth M, Simon A, et al. Mechanism-based corrector combination restores DeltaF508-CFTR folding and function. Nat Chem Biol 2013;9:444–454.
11. Ramsey BW, Davies J, McElvaney NG, Tullis E, Bell SC, Drevinek P, Griese M, McKone EF, Wainwright CE, Konstan MW, et al. A CFTR potentiator in patients with cystic fibrosis and the G551D mutation. N Engl J Med 2011;365:1663–1672.
12. Wainwright CE, Elborn JS, Ramsey BW. Lumacaftor-Ivacaftor in patients with cystic fibrosis homozygous for phe508del CFTR. N Engl J Med 2015;373:1783–1784.
13. Garmany TH, Moxley MA, White FV, Dean M, Hull WM, Whitsett JA, Nogee LM, Hamvas A. Surfactant composition and function in patients with ABCA3 mutations. Pediatr Res 2006;59:801–805.
14. Griese M, Kirmeier HG, Liebisch G, Rauch D, Stuckler F, Schmitz G, Zarbock R, Kids-Lung-Register. Surfactant lipidomics in healthy children and childhood interstitial lung disease. PLoS ONE 2015;10:e0117985.
15. Geurts AM, Yang Y, Clark KJ, Liu G, Cui Z, Dupuy AJ, Bell JB, Largaespada DA, Hackett PB. Gene transfer into genomes of human cells by the sleeping beauty transposon system. Mol Ther 2003;8:108–117.
16. Zarbock R, Kaltenborn E, Frixel S, Wittmann T, Liebisch G, Schmitz G, Griese M. ABCA3 protects alveolar epithelial cells against free cholesterol induced cell death. Biochim Biophys Acta 2015;1851:987–995.
17. Benjamini Y, Hochberg Y. Controlling the false discovery rate: a practical and powerful approach to multiple testing. J R Statist Soc B 1995;57:289–300.
18. Flamein F, Riffault L, Muselet-Charlier C, Pernelle J, Feldmann D, Jonard L, Durand-Schneider AM, Coulomb A, Maurice M, Nogee LM, et al. Molecular and cellular characteristics of ABCA3 mutations associated with diffuse parenchymal lung diseases in children. Hum Mol Genet 2012;21:765–775.
19. Griese M, Lorenz E, Hengst M, Schams A, Wesselak T, Rauch D, Wittmann T, Kirchberger V, Escribano A, Schaible T, et al. Surfactant proteins in pediatric interstitial lung disease. Pediatr Res 2016;79:34–41.
20. Tafel O, Latzin P, Paul K, Winter T, Woischnik M, Griese M. Surfactant proteins SP-B and SP-C and their precursors in bronchoalveolar lavages from children with acute and chronic inflammatory airway disease. BMC Pulm Med 2008;8:6.
21. Beers MF, Zhao M, Tomer Y, Russo SJ, Zhang P, Gonzales LW, Guttentag SH, Mulugeta S. Disruption of N-linked glycosylation promotes proteasomal degradation of the human ATP-binding cassette transporter ABCA3. Am J Physiol Lung Cell Mol Physiol 2013;305:L970–80.
22. Fitzgerald ML, Xavier R, Haley KJ, Welti R, Goss JL, Brown CE, Zhuang DZ, Bell SA, Lu N, McKee M, et al. ABCA3 inactivation in mice causes respiratory failure, loss of pulmonary surfactant, and depletion of lung phosphatidylglycerol. J Lipid Res 2007;48: 621–32.
23. He L, Kota P, Aleksandrov AA, Cui L, Jensen T, Dokholyan NV, Riordan JR. Correctors of DeltaF508 CFTR restore global conformational maturation without thermally stabilizing the mutant protein. FASEB J 2013;27:536–45.
24. Phuan PW, Veit G, Tan J, Roldan A, Finkbeiner WE, Lukacs GL, Verkman AS. Synergy-based small-molecule screen using a human lung epithelial cell line yields DeltaF508-CFTR correctors

that augment VX-809 maximal efficacy. Mol Pharmacol 2014;86:42–51.
25. Cheong N, Madesh M, Gonzales LW, Zhao M, Yu K, Ballard PL, Shuman H. Functional and trafficking defects in ATP binding cassette A3 mutants associated with respiratory distress syndrome. J Biol Chem 2006;281:9791–9800.
26. Park SK, Amos L, Rao A, Quasney MW, Matsumura Y, Inagaki N, Dahmer MK. Identification and characterization of a novel ABCA3 mutation. Physiol Genomics 2010;40:94–99.
27. Schlame M, Casals C, Rustow B, Rabe H, Kunze D. Molecular species of phosphatidylcholine and phosphatidylglycerol in rat lung surfactant and different pools of pneumocytes type II. Biochem J 1988;253:209–15.
28. Kurmann AA, Serra M, Hawkins F, Rankin SA, Mori M, Astapova I, Ullas S, Lin S, Bilodeau M, Rossant J, et al. Regeneration of thyroid function by transplantation of differentiated pluripotent stem cells. Cell Stem Cell 2015;17:527–542.
29. Hawkins F, Kotton DN. Embryonic and induced pluripotent stem cells for lung regeneration. Ann Am Thorac Soc 2015;12: S50–S53.
30. Shapiro DL, Nardone LL, Rooney SA, Motoyama EK, Munoz JL. Phospholipid biosynthesis and secretion by a cell line (A549) which resembles type II aleveolar epithelial cells. Biochim Biophys Acta 1978;530:197–207.

SUPPORTING INFORMATION

Additional supporting information may be found in the online version of this article at the publisher's web-site.